

Coherence and Superconductivity in Coupled One-Dimensional Chains: A Case Study of $\text{YBa}_2\text{Cu}_3\text{O}_y$

Y.-S Lee,¹ Kouji Segawa,² Yoichi Ando,² and D. N. Basov¹

¹*Department of Physics, University of California at San Diego, La Jolla, California 92093-0319, USA*

²*Central Research Institute of Electric Power Industry, Komae, Tokyo 201-8511, Japan*

(Received 18 May 2004; published 8 April 2005)

We report the infrared (IR) response of Cu-O chains in the high- T_c superconductor $\text{YBa}_2\text{Cu}_3\text{O}_y$ over the doping range spanning $y = 6.28$ – 6.75 . We find evidence for a power law scaling at mid-IR frequencies consistent with predictions for Tomonaga-Luttinger liquid, thus supporting the notion of one-dimensional transport in the chains. We analyze the role of coupling to the CuO_2 planes in establishing metallicity and superconductivity in disordered chain fragments.

DOI: 10.1103/PhysRevLett.94.137004

PACS numbers: 74.25.Gz, 74.72.Bk

The appeals of one-dimensional (1D) electronic systems are many. Indeed, foundational concepts of condensed matter physics are revised in the one dimension [1]. The conventional quasiparticle description breaks down in 1D solids and the spin-charge separation concept needs to be invoked to understand excitations. An experimental exploration of 1D physics spans a diversity of systems ranging from conducting molecules to unidirectional charge-ordered regions (stripes) in high- T_c superconductors and quantum Hall structures. Many aspects of 1D physics including the formation of the correlation gap in the electrodynamic response [2] are well understood in part owing to the advent of exactly solvable models [3]. An arrangement of coupled 1D conductors is envisioned as a paradigm to explain unconventional properties at higher dimensions specifically in the context to the problem of high- T_c superconductivity. While the principal building blocks of cuprate superconductors are two-dimensional CuO_2 planes, a prototypical family of high- T_c materials $\text{YBa}_2\text{Cu}_3\text{O}_y$ (YBCO) does also possess 1D elements—the so-called Cu-O chains. In (nearly) stoichiometric $y = 6.95$ and $\text{YBa}_2\text{Cu}_4\text{O}_8$ compounds chains are conducting and also show substantial contribution to the superfluid density [4,5].

Here we investigate the emergence of coherent response and superconductivity in the electrodynamics of the chains in underdoped YBCO compounds ($y = 6.28$ – 6.75). In these materials chain fragments extend over distances 15–400 Å (depending on the doping), which is insufficient to maintain dc currents across macroscopic specimens. Our infrared (IR) experiments show that when the chain fragment length exceeds a critical value their coupling via neighboring CuO_2 planes enables direct contribution of the Cu-O chains to the dc transport and superconductivity. At frequencies above the correlation gap (50–200 meV, another doping-dependent parameter) the electrodynamics of chain fragments reveals universal scaling behavior previously found in other classes of 1D conductors [6–8] in accord with predictions for the Tomonaga-Luttinger (TL) liquid. We emphasize that the interplay between super-

conductivity and the correlated insulating state is difficult to investigate in more conventional 1D systems. In this regard, YBCO compounds constitute an excellent test bed for a survey of the issues pertaining to superconductivity of 1D coupled conductors as will be elaborated below.

We investigated detwinned YBCO single crystals with oxygen content $y = 6.28, 6.30, 6.35, 6.40$ ($T_c \sim 2$ K), 6.43 ($T_c \sim 13$ K), 6.50 ($T_c \sim 13$ K), 6.55 ($T_c \sim 50$ K), 6.65 ($T_c \sim 60$ K), and 6.75 ($T_c \sim 65$ K) grown by a conventional flux method and detwinned under uniaxial pressure [9]. Annealing under the uniaxial pressure also aligns chain fragments along the b axis in nonsuperconducting YBCO ($y = 6.28$ – 6.35). Reflectivity spectra $R(\omega)$ at nearly normal incidence were measured with polarized light at frequencies from 20 to 48 000 cm^{-1} and at temperatures from 10 to 293 K. The complex optical conductivity spectra, $\tilde{\sigma}(\omega) = \sigma_1(\omega) + i\sigma_2(\omega)$, were obtained from the measured $R(\omega)$, using the Kramers-Kronig (KK) transformation. The KK-derived results are consistent with those obtained by ellipsometry. Note that the chains in the YBCO system extend along the b axis of the crystal and therefore do not contribute to the conductivity probed in the polarization $\mathbf{E} \parallel a$. On the contrary, both the CuO_2 planes and the 1D Cu-O chains jointly contribute to the b -axis spectra.

We first review the key features of the electromagnetic response of underdoped YBCO. Below the charge transfer excitation near 14 000 cm^{-1} one can identify two distinct absorption channels in the dissipative part of the conductivity. At the lowest frequencies ($\omega < 600$ cm^{-1}) one recognizes a coherent contribution that has the Drude-like form. In disordered samples where localization effects are important, the Drude mode may evolve into a resonance centered at nonzero frequency. This particular transformation is especially clear in the b -axis conductivity of the $y = 6.65$ crystal showing a resonance at 200 cm^{-1} at low T [Fig. 1(a)]. This low-frequency mode has to be contrasted with the smooth spectra of the $y = 6.75$ phase in Fig. 1(b). The coherent contribution to the conductivity is strongly T dependent and the changes of $\sigma(\omega, T)$ are

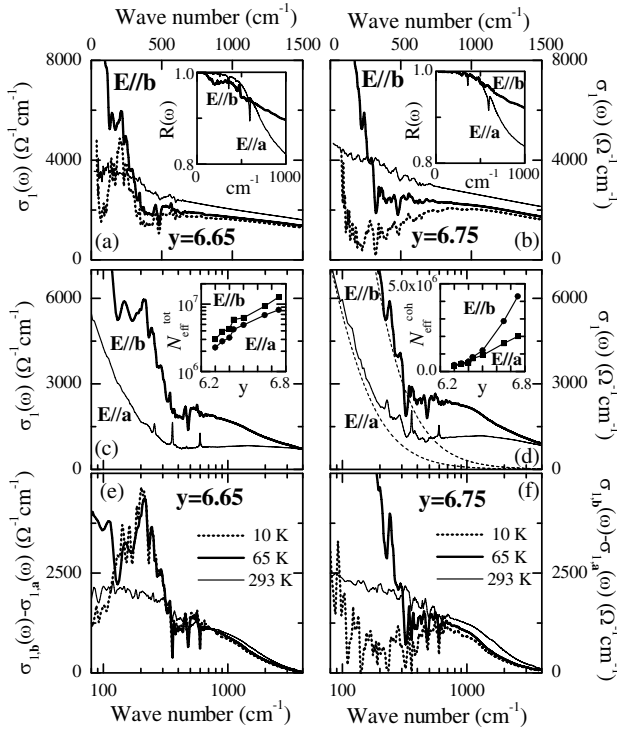


FIG. 1. Spectra of the real part of the conductivity for $y = 6.65$ (left panels) and $y = 6.75$ crystals (right panels). On the top we show the b -axis data with raw reflectivity results at 10 K displayed in the insets. Middle panels depict the a - and b -axis spectra at 65 K, along with doping dependence of the total intragap spectral weight $N_{\text{eff}}^{\text{tot}}$ [(c), left inset] and the coherent part of the spectral weight $N_{\text{eff}}^{\text{coh}}$ [(d), right inset]. In (d), the dotted lines represent the Drude fitting results for coherent modes. The fitted dc resistivity and scattering rate are 60 (35) $\mu\Omega$ cm and 75 (105) cm^{-1} for the a (b) axis, respectively. Bottom panels (e), (f) show the difference in conductivity $\sigma^{\text{ch}}(\omega) = \sigma_{1,b}(\omega) - \sigma_{1,a}(\omega)$ attributable to the response of the chains as described in the text. One finds a resonance structure centered at ~ 200 cm^{-1} in the low- T b -axis data [panels (a), (c), and (e)] for the $y = 6.65$ sample.

directly related to transport data. Apart from the coherent low- ω mode, a broad absorption structure is clearly seen in the mid-IR conductivity. The mid-IR absorption does not show significant modifications with T . With increased doping both features grow in strength and can no longer be distinguished in optimally doped phases.

We now turn to the analysis of the effects in the electromagnetic response attributable to Cu-O chain fragments. It is instructive to consider various ways in which the chains influence charge dynamics by introducing the electronic spectral weight $N_{\text{eff}}(\omega) = \int_0^\omega \sigma_1(\omega') d\omega'$. In the inset of Fig. 1(c) and 1(d), we show the doping dependence of the total intragap spectral weight $N_{\text{eff}}^{\text{tot}} = N_{\text{eff}}(\omega = 10000 \text{ cm}^{-1})$ and that of the coherent component alone $N_{\text{eff}}^{\text{coh}} = N_{\text{eff}}(\omega = 600 \text{ cm}^{-1})$ separately for the a -axis and b -axis data. A quick inspection of the plots shows that the chains increase the total spectral weight registered in the

b -axis conductivity by as much as $\sim 40\%$ in all underdoped samples in accord with the earlier data [10]. The doping dependence of the coherent spectral weight is different: $N_{\text{eff}}^{\text{coh}}$ is nearly isotropic for $y \leq 6.50$, but at higher dopings $N_{\text{eff}}^{\text{coh}}$ acquires anisotropy that is progressively increasing with y . An enhancement of the $N_{\text{eff}}^{\text{coh}}$ in the b -axis response may be attributed to the *direct* contribution of the Cu-O chains to the far-IR conductivity [11]. We stress that the anisotropy of the coherent contribution is observed only when the doping exceeds a critical value above $y = 6.50$ for this set of samples. X-ray, NMR, and optical experiments convincingly show that the length of the chain segments is progressively increasing with doping [12–14]. Given this trend, we therefore conclude that a minimum length of chains is required to trigger the coherent component [15].

It is useful to supplement the analysis of the anisotropy of the electronic spectral weight with the examination of $\sigma^{\text{ch}}(\omega) = \sigma_{1,b}(\omega) - \sigma_{1,a}(\omega)$. Assuming that the chains produce a parallel conductivity channel in YBCO, the spectra of $\sigma^{\text{ch}}(\omega)$ are attributable to the response of the chains [10]. For $y \leq 6.50$, in accord with the N_{eff} analysis discussed above, the $\sigma^{\text{ch}}(\omega)$ reveal no significant electronic contribution below 600 cm^{-1} [top panel of Fig. 2(a)]. The dominant chain contribution to optical conductivity in these samples is an asymmetric mid-IR mode revealing considerable softening with the increase of y . The similar structure at lower ω can be identified in the $\sigma^{\text{ch}}(\omega)$ data for both the $y = 6.65$ and 6.75 crystals. In addition, we have been able to detect significant low-frequency conductivity in the latter compounds, uncovering interesting T dependence [bottom panel of Fig. 1]. The low- ω coherent response of the chains above T_c in the $y = 6.75$ sample leads to $\sigma^{\text{ch}}(\omega)$ that is monotonically increasing as $\omega \rightarrow 0$, whereas the dominant contribution to the low T $\sigma^{\text{ch}}(\omega)$ for the $y = 6.65$ compound is a narrow resonance at 200 cm^{-1} .

We now focus on the analysis of the mid-IR mode in the $\sigma^{\text{ch}}(\omega)$ spectra. The bottom panel of Fig. 2 shows the scaling behavior of this mode. The diagram demonstrates that all spectra collapse on a single curve following $\omega/\omega_{\text{peak}}$ protocol for the abscissa and $\sigma^{\text{ch}}(\omega)/\sigma_{\text{peak}}^{\text{ch}}$ renormalization for the vertical axis. Here, ω_{peak} and $\sigma_{\text{peak}}^{\text{ch}}$ represent the position and the height of the mid-IR mode, respectively. The scaling behavior persists up to ~ 0.5 eV and is obeyed for the variation of ω_{peak} from 650 cm^{-1} for $y = 6.75$ to 2500 cm^{-1} for $y = 6.30$ [16], attesting to the significance of this result. Although the gross features of the a -axis conductivity of YBCO and other cuprates are similar to those seen in the $\sigma^{\text{ch}}(\omega)$ spectra, the scaling trend is not identified in the a axis. We therefore conclude that physics underlying the scaling law is intimately related to the 1D character of the electronic transport in the chains. This conjecture is supported by theoretical analyses of the optical conductivity of 1D correlated insulators within the

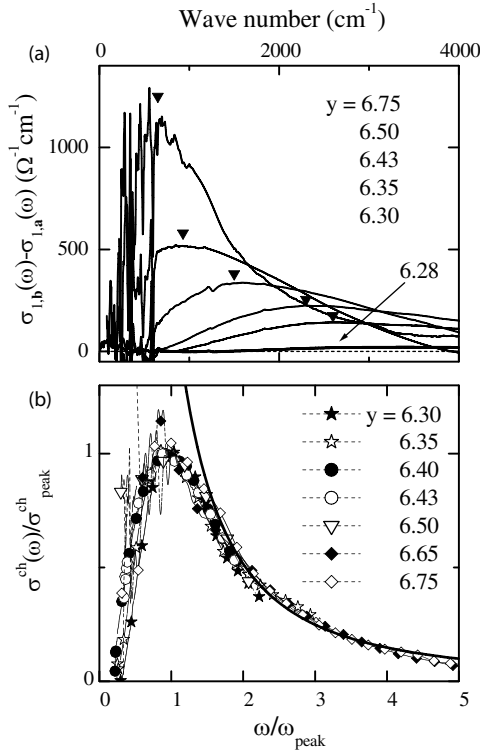


FIG. 2. (a) Spectra of $\sigma^{\text{ch}}(\omega) = \sigma_{1,b}(\omega) - \sigma_{1,a}(\omega)$ at lowest temperatures for a series of YBCO crystals. For $y = 6.75$, the coherent mode is not visible because its weight is transferred to superconducting δ peak at $\omega = 0$. (b) $\sigma^{\text{ch}}(\omega)/\sigma_{\text{peak}}^{\text{ch}}$ with $\omega/\omega_{\text{peak}}$ as the abscissa. For clarity, the sharp phonon structures are removed from the data in the bottom panel. The solid line represents $\omega^{-\alpha}$ dependence with $\alpha = 1.6$.

TL theory [2,3]. These models prescribe the emergence of a correlation gap E_g in a 1D system near commensurate fillings leading to a strong asymmetric resonance in the $\sigma(\omega)$ at E_g . When the filling deviates from the commensurability due to doping, a coherent mode is expected to emerge within the correlation gap. Hence, a salient feature of the metal-insulator transition in a correlated 1D system is the development of a *two-component* form of the optical conductivity. Remarkably, the spectra of $\sigma(\omega)$ for $\omega > E_g$ are predicted to follow the same power law $\sigma(\omega) \propto \omega^{-\alpha}$ behavior on both metallic and insulating sides of the transition. Thus the gross features of the electromagnetic response attributable to 1D Cu-O chains as well as the evolution of these trends with doping are consistent with the predictions of the TL theory.

Hallmarks of one-dimensionality uncovered by the above analysis of the $\sigma^{\text{ch}}(\omega)$ spectra motivate us to compare electrodynamics of the Cu-O chains with the behavior of more conventional 1D conductors complying with the predictions of the TL model. The observed power law with $\alpha = 1.6$ in Fig. 2 is distinct from the ω^{-3} response expected for a band insulator [2], but is close to $\alpha = 1.3$ seen in 1D Bechgaard salts [6,7]. The range of E_g values in

YBCO is comparable to that of the Bechgaard salts as well [6,7]. An important feature of the TL model is that universal 1D scaling characteristics are expected to be found only at frequencies above E_g whereas at lower energies ($\omega < E_g$) a system of coupled 1D conductors shows 2D or 3D behavior [2,17]. This dimensional crossover is seen in Bechgaard salts [2,6,7] and also can be identified in the $\sigma^{\text{ch}}(\omega)$ data for YBCO crystals with $y > 6.50$ revealing a prominent coherent contribution. Notably, the low-energy properties of the TL liquid are nonuniversal since this behavior critically depends on the details of the interchain coupling. An important aspect of the coupling in YBCO is a close proximity of the chains to the CuO_2 planes implying that the hybridization between the chain and plane states has to be taken into account [18]. This strong coupling is likely to be responsible for the pronounced spectral weight of the coherent mode relative to the total weight in the $\sigma^{\text{ch}}(\omega)$ spectra. Indeed, we find that for YBCO $N_{\text{eff}}^{\text{coh}}/N_{\text{eff}}^{\text{tot}} \sim 40\text{--}50\%$ whereas in Bechgaard salts this ratio is as small as 1–2% [6,7]. Given the strong chain-to-plane coupling when CuO_2 layers may act as Ohmic heat baths for charge degrees of freedom [19], it is not surprising that the power laws close to the Fermi liquid pattern seen in the T dependence of the chain resistivity $\rho^{\text{ch}}(T) [= 1/(\sigma_b - \sigma_a)]$ [20] are different from those observed in 1D organic conductors.

We now turn to the analysis of the transformation of the spectra in the superconducting state. A spectroscopic signature of superconductivity is the transfer of the electronic spectral weight from finite frequencies to superconducting δ function at $\omega = 0$. The strength of the $\delta(0)$ peak referred to as the superfluid density ρ_s can be readily evaluated from the so-called missing area in the conductivity data, following the Ferrel-Glover-Tinkham sum rule: $\rho_s = 8 \int d\omega [\sigma_1(\omega, T > T_c) - \sigma_1(\omega, T \ll T_c)]$ or from the imaginary part of the conductivity [21]. Data in the top panel of Fig. 3 uncover nearly isotropic ρ_s in the $y = 6.65$ crystal, whereas for $y = 6.75$ the superconducting condensate is strongly enhanced in the b -axis data. This contrasting behavior of the two crystals can be traced back to distinctions in the low-frequency coherent contribution to $\sigma^{\text{ch}}(\omega)$ at $T \simeq T_c$. Indeed, in the $y = 6.75$ crystal one finds a Drude-like form of the low- ω conductivity whereas in the $y = 6.65$ sample the coherent contribution produces a finite energy resonance centered at 200 cm^{-1} . Similar absorption structures are commonly found in the optical conductivity data for low-dimensional disordered conductors, and can be attributed to the weak localization induced by defects or disorders [22]. Apparently, bound carriers forming a 200 cm^{-1} resonance are excluded from contributing to ρ_s . We also plotted the y -dependent ρ_s from $y = 6.50$ to 6.95 [5]. Data in Fig. 3 show that ρ_s along the b axis starts to exceed that probed along the a axis for $y > 6.65$, coincident with the disappearance of the localization mode at 200 cm^{-1} . Evidently, the delocalization of the bound

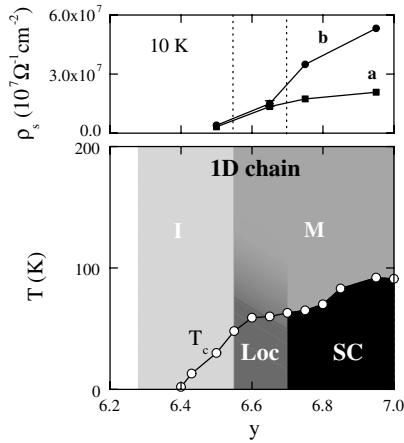


FIG. 3. Top panel: the doping dependence of the superfluid density ρ_s at $y = 6.50$ – 6.95 [5] separately for a -axis and b -axis data. Bottom panel: phase diagram displaying characteristic regimes in the response of the Cu-O chains. Here I stands for insulating, LOC for localized metal, M for Drude metal, and SC for superconducting.

carriers yields an additional contribution to the superfluid density resulting in anisotropic ρ_s in YBCO.

The experiments detailed above uncover several new facets of the response of 1D conducting elements in the environment of doped Mott-Hubbard insulators. The scaling behavior of $\sigma^{\text{ch}}(\omega)$ reaffirms the applicability of the TL description to the response of the Cu-O chains segments in YBCO. Our measurements indicate that the chain segment length has to exceed a minimum value (15–20 Å) to trigger the universal power law in $\sigma(\omega)$ data [12,13]. Indeed, no readily identifiable resonance is found in the data for the $y = 6.28$ crystal which has an average length of Cu-O segments below this cutoff [Fig. 2(a)]. The proximity to highly conducting CuO_2 planes defines an entirely different character of the coherent mode in the $\sigma^{\text{ch}}(\omega)$ spectra. Specifically, the plane-mediated processes dramatically enhances the strength of the coherent mode compared to modes generated by the direct interchain hopping in conventional 1D systems. Once the chain fragment length exceeds the critical value and the separation between these fragments is reduced, the $\sigma^{\text{ch}}(\omega)$ spectra reveal the Drude-like metallic behavior which would be impossible in a system of isolated disordered chains. In between these two regions one finds a territory marked as “localized metal” where chains do contribute to the electronic conductivity but not to the superfluid density. The superconducting condensate emerges as soon as the interchain coupling is strong enough to support conventional Drude-like behavior at $T \approx T_c$. The particular dopings corresponding to the transitions from the insulator to the localized metal and to metal in $\sigma^{\text{ch}}(\omega)$ are likely to be sensitive to details of sample preparation. Due to the effective hybridization between the plane and the chain states, the superconductivity residing in the chain might have three-

dimensional character rather than one-dimensional. Recall that the usual description of superconductivity in the chains via a proximity coupling to the planes has difficulties in accounting for the identical T dependence of the superfluid density measured along the a and b axis in YBCO [23]. In this context it is interesting to note that a superconducting ground state is one of possible ordered phases predicted to arise from interchain interaction within the TL model [2]. This corollary of the TL scenario warrants further analysis of the superconducting response of the chains using a variety of relevant probes. The doping-dependent trend in chains is reminiscent of the superconductor-insulator transition in disordered CuO_2 planes [24].

This research was supported by the US DOE.

-
- [1] M. Dressel, *Naturwissenschaften* **90**, 337 (2003).
 - [2] T. Giamarchi, *Physica B (Amsterdam)* **230**, 975 (1997), and references therein.
 - [3] D. Controzzi *et al.*, *Phys. Rev. Lett.* **86**, 680 (2001).
 - [4] Yoichi Ando *et al.*, *Phys. Rev. Lett.* **88**, 137005 (2002).
 - [5] D.N. Basov *et al.*, *Phys. Rev. Lett.* **74**, 598 (1995).
 - [6] A. Schwartz *et al.*, *Phys. Rev. B* **58**, 1261 (1998).
 - [7] V. Vescoli *et al.*, *Science* **281**, 1181 (1998).
 - [8] K. Takenaka *et al.*, *Phys. Rev. Lett.* **85**, 5428 (2000).
 - [9] Kouji Segawa and Yoichi Ando, *Phys. Rev. Lett.* **86**, 4907 (2001).
 - [10] S.L. Cooper *et al.*, *Phys. Rev. B* **47**, 8233 (1993).
 - [11] In the heavily underdoped region ($y = 6.30$ – 6.43), the dc conductivity shows a strong anisotropy in spite of the negligible anisotropy in $N_{\text{eff}}^{\text{coh}}$ [4]. This effect is *not* associated with the direct contribution of the chains to the conductivity but is instead assigned to charge modulation in the CuO_2 planes by imprinting of the charge modulation from the chain fragments as discussed in Ref. [12].
 - [12] Y.-S. Lee *et al.*, *Phys. Rev. B* **70**, 014518 (2004).
 - [13] R. Liang *et al.*, *Physica C (Amsterdam)* **383**, 1 (2002); Z. Yamani *et al.*, *Physica C (Amsterdam)* **405**, 227 (2004).
 - [14] R. Liang *et al.*, *Physica C (Amsterdam)* **336**, 57 (2000).
 - [15] It is known that details of sample preparation may strongly influence the chain length and its estimates in the literature for $y \sim 6.50$ range from 200 Å [13] to 400 Å [14].
 - [16] In a system close to quarter filling, the E_g decreases with bandwidth W increasing. The strong decrease of the E_g in the chains of YBCO indicates the gradual increase of W with y .
 - [17] E. W. Carlson *et al.*, cond-mat/0206217.
 - [18] W. A. Atkinson, *Phys. Rev. B* **59**, 3377 (1999).
 - [19] D. K. Morr and A. V. Balatsky, *Phys. Rev. Lett.* **87**, 247002 (2001).
 - [20] Robert Gagnon *et al.*, *Phys. Rev. B* **50**, 3458 (1994).
 - [21] S. V. Dordevic *et al.*, *Phys. Rev. B* **65**, 134511 (2002).
 - [22] W. Götze *et al.*, *Phys. Rev. Lett.* **35**, 1359 (1975); K. Lee *et al.*, *Phys. Rev. B* **52**, 4779 (1995).
 - [23] W. A. Atkinson and J. P. Carbotte, *Phys. Rev. B* **52**, 10601 (1995).
 - [24] D.N. Basov *et al.*, *Phys. Rev. Lett.* **81**, 2132 (1998).